REPORT DOCUMENTATION PAGE

Public Reporting burden for this collection of information is estimated to average 1 hour per response, including the time for reviewing instructions, searching existing data sources, gathering and maintaining the data needed, and completing and reviewing the collection of information. Send comment regarding this burden estimates or any other aspect of this collection of information, including suggestions for reducing this burden, to Washington Headquarters Services, Directorate for information Operations and Reports, 1215 Jefferson Davis Highway, Suite 1204, Arlington, VA 22202-4302, and to the Office of Management and Budget, Paperwork Reduction Project (0704-0188,) Washington, DC 20503.

1. AGENCY USE ONLY (Leave Blank)	2. REPORT DATE 22 May 2002	3. REPORT TYPE AND DATES COVERED Final Progress Report 15 April 1998-30 September 2001

4. TITLE AND SUBTITLE Stress Wave Propagation Through Heterogeneous Media	5. FUNDING NUMBERS DAAG55-98-1-0237 P-38081-EG

6. AUTHOR(S)
Guruswami Ravichandran

7. PERFORMING ORGANIZATION NAME(S) AND ADDRESS(ES) California Institute of Technology Graduate Aeronautical Laboratories Pasadena, CA 91125	8. PERFORMING ORGANIZATION REPORT NUMBER GR-ARO-02-01

9. SPONSORING / MONITORING AGENCY NAME(S) AND ADDRESS(ES) U. S. Army Research Office P.O. Box 12211 Research Triangle Park, NC 27709-2211	10. SPONSORING / MONITORING AGENCY REPORT NUMBER

11. SUPPLEMENTARY NOTES
     The views, opinions and/or findings contained in this report are those of the author(s) and should not be construed as an official Department of the Army position, policy or decision, unless so designated by other documentation.

12 a. DISTRIBUTION / AVAILABILITY STATEMENT Approved for public release; distribution unlimited.	12 b. DISTRIBUTION CODE

13. ABSTRACT (Maximum 200 words)

     In heterogeneous media, scattering due to interfaces/microstructure between dissimilar materials could play an important role in shock wave dissipation and dispersion. In this work the influence of interface scattering on finite-amplitude shock waves was experimentally investigated by impacting flyer plates onto periodically layered polycarbonate/6061 aluminum, polycarbonate/304 stainless steel and polycarbonate/glass composites. Experimental results (obtained using velocity interferometer and stress gage) show that periodically layered composites investigated can support steady structured shock waves. Due to interface scattering, the effective shock viscosity increases with the increase of interface impedance mismatch, and decreases with the increase of interface density (interface area per unit volume) and loading amplitude. The strain rate within the shock front for the composites studied increasing by about the square of the shock stress, comparing with the increasing by the fourth power of the shock stress for homogeneous metals, indicates that layered composites have much larger shock viscosity due to the interface/microstructure scattering. Experimental results also show that due to the scattering effects, shock propagation in the layered composites is dramatically slowing down and the shock speed in composites can be lower than that of either its components.

14. SUBJECT TERMS Solid Mechanics; shock waves; heterogeneous materials; experimental mechanics	15. NUMBER OF PAGES 21
	16. PRICE CODE

17. SECURITY CLASSIFICATION OR REPORT **UNCLASSIFIED**	18. SECURITY CLASSIFICATION ON THIS PAGE **UNCLASSIFIED**	19. SECURITY CLASSIFICATION OF ABSTRACT **UNCLASSIFIED**	20. LIMITATION OF ABSTRACT **UL**

NSN 7540-01-280-5500

GENERAL INSTRUCTIONS FOR COMPLETING SF 298

The Report Documentation Page (RDP) is used for announcing and cataloging reports. It is important that this information be consistent with the rest of the report, particularly the cover and title page. Instructions for filling in each block of the form follow. It is important to *stay within the lines* to meet *optical scanning requirements.*

Block 1. Agency Use Only (Leave blank)

Block 2. Report Date. Full publication date including day, month, and year, if available (e.g. 1 Jan 88). Must cite at least year.

Block 3. Type of Report and Dates Covered. State whether report is interim, final, etc. If applicable enter inclusive report dates (e.g. 10 Jun 87 - 30 Jun 88).

Block 4. Title and Subtitle. A title is taken from the part of the report that provides the most meaningful and complete information. When a report is prepared in more than one volume, repeat the primary title, and volume number, and include subtitle for the specific volume. On classified documents enter the title classification in parentheses.

Block 5. Funding Numbers. To include contract and grant numbers; may include program element number(s) project number(s), task number(s), and work unit number(s). Use the following labels:

C	- Contract	**PR**	- Project
G	- Grant	**TA**	- Task
PE	- Program Element	**WU**	- Work Unit Accession No.

Block 6. Author(s). Name(s) of person(s) responsible for writing the report, performing the research, or credited with the content of the report. If editor or compiler, this should follow the name(s).

Block 7. Performing Organization Name(s) and Address(es). Self-explanatory.

Block 8. Performing Organization Report Number. Enter the unique alphanumeric report number(s) assigned by the organization performing the report.

Block 9. Sponsoring/Monitoring Agency Name(s) and Address(es) Self-explanatory.

Block 10. Sponsoring/Monitoring Agency Report Number. (*if known*)

Block 11. Supplementary Notes. Enter information not included elsewhere such as; prepared in cooperation with....; Trans. of...; To be published in.... When a report is revised, include a statement whether the new report supersedes or supplements the older report.

Block 12a. Distribution/Availability Statement. Denotes public availability or limitations. Cite any availability to the public. Enter additional limitations or special markings in all capitals (e.g. NORFORN, REL, ITAR).

DOD	-	See DoDD 4230.25, "Distribution Statements on Technical Documents."
DOE	-	See authorities.
NASA	-	See Handbook NHB 2200.2.
NTIS	-	Leave blank.

Block 12b. Distribution Code.

DOD	-	Leave Blank
DOE	-	Enter DOE distribution categories from the Standard Distribution for unclassified Scientific and Technical Reports
NASA	-	Leave Blank.
NTIS	-	Leave Blank.

Block 13. Abstract. Include a brief (*Maximum 200 words)* factual summary of the most significant information contained in the report.

Block 14. Subject Terms. Keywords or phrases identifying major subject in the report.

Block 15. Number of Pages. Enter the total number of pages.

Block 16. Price Code.   Enter appropriate price code (NTIS *only*).

Block 17. - 19. Security Classifications. Self-explanatory. Enter U.S. Security Regulations (i.e., UNCLASSIFIED). If form contains classified information, stamp classification on the top and bottom of the page.

Block 20. Limitation of Abstract. This block must be completed to assign a limitation to the abstract. Enter either UL (Unlimited) or SAR (same as report). An entry in this block is necessary if the abstract is to be limited. If blank, the abstract is assumed to be unlimited.

REPORT DOCUMENTATION PAGE (SF298)
(Continuation Sheet)

Table of Contents

1. Background

Shock wave propagation and its effects on solids have been extensively investigated in the past few decades (Davison and Graham, 1979; Asay and Shahinpoor, 1993; Meyers, 1994). Mathematically, the front of a shock wave can be, and has customarily been, treated as a discontinuity with zero rise time, but the real shock front always has a finite rise time (for metals, ranging from several to hundreds of nanoseconds) corresponding to the compression of the material from its initial state to the final shocked state, and the slope of the shock front varies with shock amplitude. One common interpretation for the observed finite rise-time in the steady structured shock waves propagating in homogeneous metals is that the underlying physics of time-dependent plasticity processes (dislocations, twinning, etc.) are responsible for dissipation and dispersion of the waves. Based on the formalisms of viscoplasticity, many descriptive constitutive models have been developed and are reasonably successful in interpreting the experimental data (Swegle and Grady, 1985; Rubin, 1990; Partom, 1990; Johnson, 1992).

Wave propagation in heterogeneous solids has received considerable attention and earlier efforts have resulted in a sound understanding of many fundamental issues. Nevertheless, most of the consequences of wave dispersion in composite materials were brought to light through investigations of the linear elastic analysis of ideal periodic composites (Sun, et al., 1968; Ben-Amoz, 1975; Nayfeh, 1995). Relatively little is known regarding finite amplitude shock wave propagation in heterogeneous media. Much of the attention of the earlier work has been on the geometric dispersion of elastic waves, almost no insight exists concerning the role of interface scattering effects on the dispersion and dissipation of shock (finite amplitude) waves in heterogeneous solids. So far, only a limited number of experiments have been carried out that are concerned with finite-amplitude wave propagation in composite materials for the loading stress in the intermediate regime, where strength effects are relevant. Barker et al. (1974) conducted experiments on periodic laminates and found that below certain critical input amplitude, the stress wave amplitude decayed exponentially with distance and formed a structured shock wave above that critical amplitude. Lundergan and Drumheller (1971) and Oved et al. (1978) also conducted limited shock wave experiments on layered stacks, which showed resonance phenomena due to layering. There has been a lack of systematic experimental study of stress wave propagation in either layered systems or fiber reinforced composites, which would be valuable in development or validation of physically based models for transient (pulse) loading.

Theoretical models for predicting the structure of the profile of shock wave propagating in composites is not yet available. A few simplified phenomenological models have been proposed by Barker (1971), Chen and Gurtin (1973), Kanel, et al. (1995), and Johnson, et al. (1994). These models account for dispersion through a time-dependent relaxation process assuming the existence of a steady shock wave. Recently, based on nonequilibrium phonon energy induced by scattering of waves within heterogeneous microstructure, Grady et al. (1999) proposed a continuum anelastic response model for finite amplitude wave propagation in the heterogeneous media. In order to validate these models, experiments on the finite-amplitude shock wave propagating in heterogeneous composites are needed to be systematically carried out to provide fundamental understanding and insight of the physics of the processes occurring during the shock compression of the heterogeneous media.

The objective of the research conducted under the ARO grant is to study the influence of scattering effects induced by internal interfaces on shock wave propagation in heterogeneous media. To do so, experiments are designed and conducted in order to evaluate the role of interface heterogeneity, i.e., impedance mismatch, multiple length scales, and the interface characteristics on stress wave dispersion and attenuation. It is expected that the results of this investigation (experiments and simulations) can establish a basis for formulating physically based constitutive models accounting for the microstructure scattering effects on the wave propagation, which can be implemented in computational codes for simulating and assessing the performance of heterogeneous systems and structures exposed to an impact related shock environment.

2.   Shock Compression Experiment

2.1.   Specimen Configuration

The structure of a periodically layered composite specimen is shown in Fig. 1. It consists of two components in the form of thin disks that are alternatively stacked together. Hereafter, the component with larger mechanical impedance is called "hard" layer, while the other with lower mechanical impedance is called "soft" layer, and the combination of a soft layer and a hard layer will be referred to as a composite "unit" or a "unit cell." The layered composite specimen for the shock compression experiment is prepared by repeating the composite unit as many times as necessary to form a specimen with desired thickness. In this study, except when stated otherwise, the composite layers are ordered in such a way that the first layer is always soft layer in a unit cell, i.e., the soft layer will be the first to experience the planar impact loading. There is no special physical or mechanical consideration as to why the soft layer should be placed first, except that the specimens were consistently prepared this way. A buffer layer of the same material as the soft component of the specimen was used after the specimen. A window in contact with the buffer layer was used to prevent the free surface from serious damage due to unloading from shock wave reflection at the free surface. The rear surface of the buffer layer or the front surface of the window was mirrorized to provide good reflectivity for velocity interferometer system (VISAR) optical measurements. The window was typically 12.7 mm in thickness and was made of polymethyl methacrylate (PMMA). The thickness of the buffer layer was typically 0.74 mm.

2.2.   Component Materials

Four different materials, polycarbonate (PC), 6061-T6 aluminum alloy (Al), 304 stainless steel (SS) and glass (GS), were chosen as components, and two thicknesses of each component layer were used except aluminum for which only one thickness was available. These materials, whose dynamic response to shock wave loading have been extensively studied and well described in the terms of their constitutive behavior (Wackerle, 1962; Fraser, 1968; Barker and Hollenbach, 1970; Marsh, 1980), provide a wide range of combinations of shock wave speeds, acoustic impedance and strength levels to develop a fundamental understanding of shock wave propagation through heterogeneous solids.

The "soft" layer in composite units was PC sheet of thickness 0.37 mm (shorted as PC37) or 0.74 mm (PC74), which were obtained from McMaster-Carr. The "hard" layer was one of the following materials: 0.20 mm thick D-263 glass (GS20), 0.55 mm thick float glass (GS55), 0.37 mm thick 6061-T6 aluminum sheet (Al37), 0.19 mm or 0.37 mm thick 304 stainless steel sheets (SS19 or SS37). The glasses were the products of Erie Scientific Company, and the 304 stainless steel sheets were from Allegheny Rodney Strip, the service center division of Allegheny Ludlum Corporation, while the 6061-T6 aluminum alloy was a commercial grade material. The window material was 12.7 mm thick commercial PMMA plate. The flyer plates were made of 2.87 mm PC plate supplied from McMaster-Carr. In a few cases, Al flyer was also used when higher stress level was desired. The mechanical properties of materials used are listed in Table 1.

The diameters of specimen and flyer were 38.1 mm and 34 mm, respectively. The component layers were machined into disks and then bonded together with the clear two-component epoxy adhesive Hysol 0151 supplied from Dexter Corporation. The average thickness of the epoxy layer bond was about 20 μm. For the PC/GS composites, the bonding layer could be as thin as 10 μm. The detail of specimen preparation was described elsewhere (Zhuang, 2002).

2.3.   Experiments

The experiments of shock compression of layered composites were conducted using a powder gun system located in the experimental solid mechanics facilities, Graduate Aeronautical Laboratories at Caltech (GALCIT) (Zhuang, 2002; Mutz, 1991). The bore of the gun is 36 mm, and flyer velocity achieved by this gun ranges from 400 m/s to about 2000 m/s. The flyer velocity is measured within ± 1% using a light interruption fiber optic system. The tilt of the flyer with respect to the specimen during impact is measured by a method called

"projectile's shorting of charged electrical probes" (Asay et al., 1993)). The average impact tilt divided by the impact velocity in this study was generally much less than 0.005 rad/mm/µs. The particle velocity history on the interface between the window and the buffer layer was measured by the so called VISAR system (Barker and Hollenbach, 1972). To detect the resonant oscillation wavelets superposing on the shock profile due to the multiple reflections from internal interfaces as a shock wave propagates in the layered composites, a high resolution VISAR with velocity fringe constant adjustable from 85 to 1,500 m/s/fringe was constructed (Zhuang, 2002). Tektronix TDS 7104 digital phosphor oscilloscope was used to record the VISAR singles.

Besides the VISAR system, manganin gages were also embedded between layers in some specimens to measure the stress history at selected internal points (see Fig. 1). The manganin gages used were 50 Ω ones produced by either Dynasen, Inc., (MN4-50-EK) or Micro Measurements (MM) Group (J2M-SS-110FB-048).

In this investigation three types of composite specimens with five different geometric configurations were prepared. The first type was a periodically layered PC/Al composite. The thicknesses of PC and Al layers were 0.74 mm and 0.37 mm, respectively, and the composite of this type is referred to as PC74/Al37. For the sake of convenience, the two numbers following the abbreviation of the material name of a component are the individual layer thickness in hundredths of a millimeter. For instance, 0.74 mm PC layer is abbreviated as PC74. The second type of composite was formed by PC and SS. Two thicknesses of each component were used, forming two structures of this type, PC74/SS37 and PC37/SS19. The third type composite was made of PC and GS layers. Again, specimens with two different thickness combinations were prepared, PC74/GS55 and PC37/GS20. The different structures of specimens and the corresponding loading conditions are summarized in Table 2. Note that the specimen thickness shown in Table 2 is the total thickness of the composite and the 0.74 mm buffer layer. From now on, unless otherwise stated, the specimen thickness refers to the total thickness of the layered composite and the 0.74 mm thick buffer, and the flyer is a PC plate of thickness 2.87 mm.

3.   Results and Discussion

3.1.   Influence of Loading Amplitude on Shock Profile

The influence of the amplitude of shock loading on the dynamic response of composites was investigated by impacting specimens with flyers at different velocities. Figure 2 shows the measured VISAR particle velocity profiles at the buffer/window interface of PC74/Al37, PC74/SS37, PC37/SS19 and PC74/GS55 composites. Notice that, for the purpose of comparison, the shock particle velocity V_p is normalized by a dimensional factor $V_f/2$, where V_f is the PC flyer velocity of the corresponding experiment, h is specimen thickness and w is the flyer thickness. Flyers were PC disks of 2.78 mm thick, otherwise, it would be marked out in the figure legend. For an 5.55 aluminum flyer at a velocity of about 1,100 m/s, the impact induced shock stress was equivalent to that achieved by a PC flyer at the velocity of about 1,600 m/s.

It can be observed that for all kinds of composites investigated, a common feature of shock velocity profiles is that the rise time of the shock front decreases with increasing flyer velocity, or in other words, the shock front steepens with the increase of shock loading strength. This indicates that the shock viscosity of the composites decreases with shock strength, which is similar to observations of shock wave propagation in homogeneous materials (Swegle and Grady, 1985).

When a single phase homogeneous material is compressed by a shock wave, the particle velocity profile typically reaches a plateau following the initial jump, i.e., the shock front, indicating the attainment of equilibrium, and is later followed by release wave which decompresses the shocked high pressure state into a low pressure state. The length of shock pulse (the plateau) is determined by the boundary conditions (flyer thickness and velocity) of the shock loading. However, when a layered heterogeneous composite is compressed by a shock wave, due to the interaction of the multiple reflections between the hard and soft layers, the plateau is generally not observable. Instead, oscillations superposed on the top of a nominal plateau is typically observed. The duration and magnitude of the oscillations depend on the geometrical length scale and the mechanical properties of each component layer, as well as the loading strength of the shock wave. It is noticed that for all the composites studied here, the magnitude of oscillation of the shock profile, especially that of the first peak, increases as the shock strength increases, while at the same time, the period of oscillation becomes shorter. Furthermore, the effect of multiple reflections of internal interfaces is not only affecting the shock

compression process, but also affecting the unloading process, which can be easily observed from the shock velocity profile of decompression process in which release progresses by multiple step-like unloading.

The influence of multiple reflections of internal interfaces on shock wave propagation in the layered composites is more clearly illustrated by the shock stress time history profiles measured by manganin gages. The manganin gages are embedded between the soft and hard layers where the stress profiles are to be measured. Figure 3 shows the comparison of shock stress profiles for PC74/SS37, PC37/SS19, PC74/GS55 and PC37/GS20 composites at different flyer velocities. The shock stress profile measured by the manganin gage is the actual shock compression process, while the particle velocity time history measured by VISAR at buffer/window interface includes the decompression effect of the release wave from the interface due to the impedance mismatch between composite and window (PMMA) materials. Comparing the measured stress profiles (e.g., Fig. 3 (b)) with the velocity profiles at the buffer/window interface (e.g., Fig. 2 (c)), it is evident that the magnitude of oscillation in the velocity profiles has been largely reduced due to the partial release at the buffer/window interface. Again, from the stress profiles in Fig. 3, it is observed that the shock profile is affected significantly by the shock loading strength, as well as the geometrical length scale and mechanical properties of each component layer.

One feature that is worth noting is that for a given loading strength, the shock front rise time of a layered composite is much longer than that of either homogeneous component material of which the composite is made. For instance, according to Fig. 2a, where the flyer velocity is 589 m/s and the corresponding particle velocity induced is about 300 m/s, the rise time of the shock front in PC74/Al37 composite is about 0.80 μs, while under similar loading condition, the shock front rise time of 6061-T6 aluminum alloy, estimated based on the experimental results by Johnson and Barker (1969), is about 20 to 30 ns if only the time of plastic wave front is considered. For PMMA, the major (initial) portion of shock front rises very rapidly and is followed by a slower compression process (Barker and Hollenbach, 1970; Schuler and Nunziato, 1974). It appears reasonable to take the rise time in PMMA to be 0.3 μs at particle velocity of 300 m/s. Since the shock compression behavior of PC is expected to be not much different from that of PMMA, it is reasonable to assume that the corresponding rise time in PC should not be longer than 0.4 μs. The much longer rise time of shock front observed in the composite indicates that the presence of the internal interfaces in heterogeneous materials enhances the dispersion effects, which affects the shock response of the composite in a way similar to the viscosity effects in viscoelastic materials.

3.2. Effects of Interface Impedance Mismatch

To study the influence of impedance mismatch of interface on shock wave propagation in heterogeneous media, layered composite specimens having the same geometrical structure, but different combinations of layer component materials, were prepared and subjected to planar impact loading at different flyer velocities. Some of the corresponding experimental results are shown in Figs. 4 and 5. Plots in Fig. 4 show the comparisons of shock velocity profiles of PC74/Al37, PC74/SS37, PC74/GS55, PC37/SS19, and PC37/GS20 composites impacted by 2.87 mm PC flyers at nominal velocity of 588 m/s or 1,050 m/s. For PC37/SS19 and PC37/GS20 composites, besides the particle velocity profiles at buffer/window interface measured using VISAR, the stress time histories of shock wave at internal interfaces were also measured by manganin gages, which are shown in the Fig. 5.

The ratios of acoustical impedance of the "hard" layer to the "soft" layer in PC/SS, PC/Al and PC/GS are approximately 23/1, 7.5/1 and 8/1, respectively. From Figs. 4 and 5, it is apparent that the interface impedance mismatch has very large effect on the structuring of the shock profiles. For a 6.45 mm thick PC74/SS37 composite, when subjected to impact loading by a PC flyer at a velocity of 588 m/s, the rise time of the shock front measured by VISAR at buffer/window interface is about 0.88 μs, while for the PC74/Al37 composite, which has less interface mechanical impedance mismatch, under the similar loading condition, the shock front rise time is about 0.47 μs (Fig. 4 (a)). When the flyer velocity is increased to about 1,050 m/s, the shock front rise times for PC74/SS37 and PC74/Al37 are 0.38 μs and 0.16 μs, respectively (Fig. 4 (b)). Therefore, the larger the impedance mismatch between the components, the longer the time that is needed for a shock front to reach its final shocked steady state. Besides affecting the shock front rise time, impedance mismatch also affects the magnitude and duration of the resonant oscillations of the shock profiles (Fig. 5), and the degree of

influence depends on the shock loading strength. When the flyer velocity is about 560 m/s, the larger the impedance mismatch, the larger the magnitude and duration of oscillations on the stress profiles. As the flyer velocity increases to 1,050 m/s, the amplitudes of oscillations of the stress profiles for both PC37/SS19 and PC37/GS20 are about the same, though the oscillation duration in the former is still larger than that in the later. The interface impedance mismatch also affects the unloading process from the shocked state, which can be seen from the release processes of the shock particle velocity profiles in Fig. 4. The PC/SS composite has larger interface impedance mismatch, its unloading process is slower than that of PC/Al or PC/GS composite and the final released state also has a higher residual particle velocity.

3.3. Influence of Interface Number on Shock Profile

To investigate the effect of interface number on shock profile, specimens of PC/SS and PC/GS composites were prepared in two geometrical structures: PC37/SS19 and PC74/SS37 for PC/SS type composites, and PC37/GS20 and PC74/GS55 for PC/GS type composites. The typical experimental results are compared respectively in Fig. 6 and Fig. 7 for particle velocity profiles and shock stress profiles.

It can be seen that for both composites the shock front steepens as the number of interfaces (density) doubles, which implies that the nonlinearity of composite increases with increasing number of interfaces. At first glance, this change in property is very similar to that of the effect of reduction in interface impedance mismatch on the shock profile, since in both cases the shock front rise time and the duration of resonant oscillations superposed on the shock profiles are decreased. But, examining in more detail, some differences can be easily observed by comparing the shock velocity profiles in Fig. 6 with those in Fig. 4. In the case where the shock front steepens due to reduction of interface impedance mismatch between components, the magnitude of the shock particle velocity profile remains the same or increases. For almost all cases shown in Fig. 4, the final released state of composites with lesser impedance mismatch has lower particle velocity. However, in the case where the interface number is doubled, the magnitude of the wave profiles tends to decrease and the particle velocity in the final released state is not significantly different from the previous two cases. This indicates that the dispersion of shock energy due to the interface has a more dominant effect than the material nonlinearity at lower shock pressures. With increasing shock pressure, the nonlinearity of the material increases. It is expected that the difference between the shock profiles of two composites, which contain different densities of interfaces, will become smaller at higher impact velocities and will eventually disappear at extremely high amplitude shock loading.

Figure 7 shows the comparisons of shock stress profiles of the two PC/GS composites, which clearly indicate that besides the influence on the shock compression process (rise time of the shock front), the interface density of composites also affects the structure of the shock profile. When the interface density doubles, the frequency of the resonant oscillations due to the multiple reflections is also increased. It is also noted that as the shock loading increases, the relative amplitude of oscillations also increases. Hence, it can be concluded that the duration of oscillation in the shock profile is determined by interface density, while the amplitude is dominated by both material properties of the components and the shock loading strength.

3.4. Evolution of Shock Profile with Propagation Distance

Figure 8 shows the evolution of shock particle velocity profiles with wave propagation distance in PC/SS composites. For the purpose of comparison, the profiles measured for different thickness specimens are shifted to the same starting point. Figure 8(a) shows the comparison of measured shock particle velocity profiles at buffer/window interface of 6.45 mm and 9.9 mm thick PC74/SS37 specimens loaded by 2.87 mm PC flyers at velocities of 550 m/s. Figure 8(b) shows the same comparison of velocity profiles for 3.7 mm, 7.1 mm and 10.5 mm thick PC37/SS19 composites loaded by the 2.87 mm PC flyers at velocities of 550 m/s. The situation is similar for composites loaded at higher flyer velocities.

Figures 9(a) and (b) are the shock stress profiles at interfaces of 3.44 mm and 6.5 mm away from impact surface for the 10.2 mm and 10.6 mm thick PC37/SS19 specimens impacted by 2.87 mm flyers at velocities of 564 m/s and 1,043 m/s, respectively. Again, the evolution of shock stress profiles inside the PC37/GS20 and

PC74/GS55 composites, impacted by 2.87 mm PC flyers at velocities of 560 m/s and 1,070 m/s, are similar to that of corresponding stress profiles in PC37/SS19 composites shown in Fig. 9(a) and (b).

From the shock profiles shown in Figs. 8 and 9, a common feature emerges: the initial compression process of the composites (within shock front) is independent of the propagation distance in the composites, indicating that a structured steady wave, or a quasi-steady wave if not strictly steady, can be achieved and propagated in the layered composites, at least it is the case for the composites investigated here. For all cases studied, the difference between the shock profiles becomes important only after the initial compression. Two mechanisms may be responsible for this difference. One is due to the dispersion resulting from the multiple reflections of interface to the shock wave, or the scattering of the internal interface to the shock wave. The other is due to the release wave originating from the rear (free) surface of the flyer and its interaction with the propagating shock wave in the composite.

Comparing the shock particle velocity profiles in Fig. 8 (which includes the partial decompression influence from the window) with the shock stress profiles in Fig. 9 (which is essentially a structured steady wave propagating inside the composites without being disturbed by any release wave except the unloading), it may be concluded that the effect of the scattering of interface to the decompression (release) wave is even more pronounced since the difference between particle velocity profiles for different thickness of specimens at same loading condition is apparent (see Fig. 8). By comparing Fig. 8(a) with 8(b) , it is worth noting that the dispersion due to interface scattering is more pronounced in the composite with smaller density of interfaces than in the composite with higher interface density, since the peak attenuation of shock profiles in the former (Figs. 8(a)) is larger than those in the latter (Figs. 8(b)).

3.5.　Influence of Pulse Duration on Propagation of Shock Waves

To investigate how the pulse duration affects the shock wave propagation in layered composites, shock compression experiments were carried out by impacting flyers of different thickness, at the same velocity, on specimens of same thickness. Figure 10 shows the shock particle velocity profiles for 3.7 mm and 10.6 mm thick PC37/SS19 specimens loaded by flyers of thickness 2.87 mm and 5.63 mm at velocity of about 1,050 m/s. The corresponding shock stress profiles for the 10.6 mm thick PC37/SS19 composites are shown in Fig. 11. The initial pulse duration generated by the 5.63 mm and 2.87 mm PC flyers at velocity of 1,050 m/s is about 3.6 μs and 1.8 μs, respectively. To obtain shorter pulse duration, say 0.5 μs, in principle, it can be achieved by reducing the thickness of the PC flyer to about 0.8 mm. But, in practice, if the polymeric flyer is thinner than 1.0 mm, it will most likely bow out backwards when it is accelerated in the barrel of the powder gun. The impact of a specimen by a curved flyer will result in a non-planar shock front in the specimen. To obtain a shorter shock pulse and avoid the problem of bowing out, a 1.20 mm aluminum flyer was accelerated to a velocity of 657 m/s impacting a PC37/SS19 specimen. The shock pulse duration generated by this Al flyer was about 0.4 μs and the shock pressure was about the same as that achieved by impacting of a PC flyer at velocity of 1,050 m/s. The corresponding shock particle velocity at buffer/window interface is compared with others in Fig. 10(b).

It can be seen from Fig. 11 (also in Fig. 10) that as a shock wave propagates in the layered PC37/SS19 composites, the compression process within the shock front does not depend on its pulse duration. Even in the case of a specimen loaded by a very short pulse (0.4 μs duration), when its front is overtaken by the release wave from the rear (free) surface of the flyer, it affects the attenuation of the shock amplitude, but not the slope of the front (Fig. 10(b)). This indicates that the layered composite does indeed support steady shock waves.

.3.6.　Influence of Release Wave from Window on Shock Profile

It is possible to measure the particle velocity history by VISAR at an internal interface of PC/GS type composites without using a window since both components, PC and GS, are optically transparent. A PC74/GS55 specimen of total thickness 20.54 mm (15 units plus a buffer layer) was prepared in the same way as for others. The interface located at 9.92 mm away from the impact surface was aluminized to be a mirror surface, which was the exact position of the buffer/window interface of a PC74/GS55 specimen with window. The laser beam for VISAR was focused on the internal mirror surface. The specimen was loaded by a 2.87 mm

thick PC flyer at a velocity of 568 m/s. In this case, the measured particle velocity time history was the shock profile at an interior location of specimen without being affected by the release wave from the buffer/window interface. The shock profile obtained in this experiment is compared in Fig. 12 with that obtained for the specimen with the window under nominally the same conditions.

It can be seen that the release wave from buffer/window interface does affect the shock profile. The influence is evident not only on the oscillatory portion of the shock profile, but also on the slope of the shock front. When a shock wave is partially released by a tensile wave traveling in the opposite direction, the front of velocity profile rises faster since the tensile wave accelerates a particle in the direction opposite to its own travelling direction. Therefore, the front of the shock wave in the specimen with window is steeper than in the transparent specimen with internal mirror. This is attributed to the release wave originating from the buffer/window interface due to the mechanical impedance mismatch. Also, this release wave from the window tends to subdue the oscillations resulting from the scattering of the shock wave by internal interfaces. The magnitude of the oscillation in the shock profile of the specimen with window is much smaller than that of the specimen without window. It is expected that the shock particle velocity profile at the internal interface should resemble the shock stress profile measured by manganin gages at the interface. This is verified by plotting the stress and velocity profiles together as shown in Fig. 13. The stress and velocity profiles are normalized by their own maxima for the purpose of comparison. The difference in the slope of the shock front between the stress and velocity profiles is attributed to the phase shift between the shock velocity profile and shock stress profile, which is caused by the interface scattering, i.e., the interaction of multiple reflected waves with the shock wave (Zhuang, 2002).

3.7. Influence of Interface Scattering on Shock Velocity and Viscosity

The experimentally measured shock Hugoniot data are summarized in Fig. 14. The Hugoniots of each components constituted the composites are also plotted in the figure for comparison. One may expect that the shock velocity of a composite (or mixture) should fall in the range bounded by the Hugoniots of its two components. However, the experimental results indicated that the shock velocity of a composite could be between the shock Hugoniots of its two components (e.g., PC/GS composites shown in Fig. 14), or even lower than the Hugoniots of both its components (e.g., PC/SS composite shown in Fig. 14). The physical mechanism of a shock wave slowing down in composites is inherently related to the interaction of multiple reflected waves from the internal interfaces with the wave, i.e., the scattering effects of internal interface on the shock wave. The details of the processes of interaction of reflected waves with incident shock wave will be explored elsewhere.

From experimental data obtained, the shock front strain rates and their corresponding shock stress were calculated and plotted in Fig. 15. Roughly, shock front strain rate ($\dot{\varepsilon}$) increases as a square of the shock stress (s), or, $\dot{\varepsilon} \propto s^n$, where $n \approx 1.8$-2.4. While, for many common metals such as Al, Fe, Be, Bi, Cu and U, $n \approx 4$, even for fused silica and MgO, $n \approx 4$ seems still true, in the stress range of one to tens of GPa (Sweglel and Grady, 1985). Based on the available data, it is estimated that for the component materials used here, roughly, $n \approx 4$ are all true(Zhuang, 2002). This means due to the interface scattering the shock front in the composite will take much longer time to reach its maximum stress under the same loading strength, indicating larger shock viscosity induced in the layered composites being compressed.

4.   Summary and Conclusions

In this experimental investigation of shock wave propagation in the periodically layered composites, three types of composite specimens with five geometric configurations were prepared and subjected to shock loading generated by planar impact. The composites that were studied include PC74/Al37, PC74/SS37, PC37/SS19, PC74/GS55 and PC37/GS20. The specimen thickness is nominally 3.7 mm, 7 mm and 10 mm. Most flyers are made of PC with 2.87 mm in thickness, and the typical flyer velocities are about 600 m/s and 1,060 m/s. Several 5.63 mm thick flyers were also used to generate shock waves with longer pulse duration. To generate higher shock loading Al flyers were also used.

In each of the experiments conducted, the VISAR system was used to obtain the shock particle velocity profiles at the buffer/window interface. In addition, manganin stress gages were also embedded in some of specimens at selected interfaces where the shock stress history and shock arrival times were of interest.

The results of this systematic experimental investigation lead to the following conclusions:

1) Periodically layered composites such as the ones used in this investigation can support steady structured shock waves.

2) The influence of internal interface on the shock wave propagation is through scattering mechanism. The interface scattering affects both bulk and deviatoric response of the composites to shock compression loading. The influence of scattering on the bulk response is to reduce the propagation velocity of shock wave, while the influence of the deviatoric response is in structuring the shock front, or in the other words, increasing the shock viscosity, which increases the shock front rise time similar to the effect of viscous material behavior in homogenous solids. In homogeneous media such as metals, the strain rate of the shock front increases by the fourth power of the shock stress, while the results of this investigation show that for layered composites, the strain rate at the shock front increases by about the square power of the shock stress, indicating much larger shock viscosity than the former.

3) With the increase of shock loading strength, the slope of the shock front increases very rapidly. At the same time the amplitude of oscillations in the wave profile also increases, which could be considered to be one of the dissipation mechanisms of the shock wave.

4) Keeping the total mass of each component unchanged, an increase in the number of interfaces (or the density of interfaces) results in (a) steepening of the shock front slope, which indicates that the nonlinearity of the composite increases, and (b) an increase in the amplitude of oscillations in the shock profile, which implies that more of the kinetic energy has been transformed to internal energy and the dissipation of shock energy increases. From Fig 14 it is seen that the shock Hugoniot curve of the composite is not sensitive to the density of interfaces, so it can be postulated that interface density plays a dominant role for the structuring of the shock front (Fig. 15).

5) Impedance mismatch between constituents at the interface also contributes to the dissipation and dispersion of the shock energy during propagation. The larger the impedance mismatch between the components, the smaller the slope of the shock front, which means the larger the dispersion. From Fig. 14 it is seen that the impedance mismatch has very strong influence on the shock wave velocity of the composite (comparing the Hugoniots of PC/SS composites with those of PC/GS ones). Therefore, it may be postulated that the interface mechanical impedance mismatch contributes to both the bulk and the deviatoric responses of the composite to shock compression.
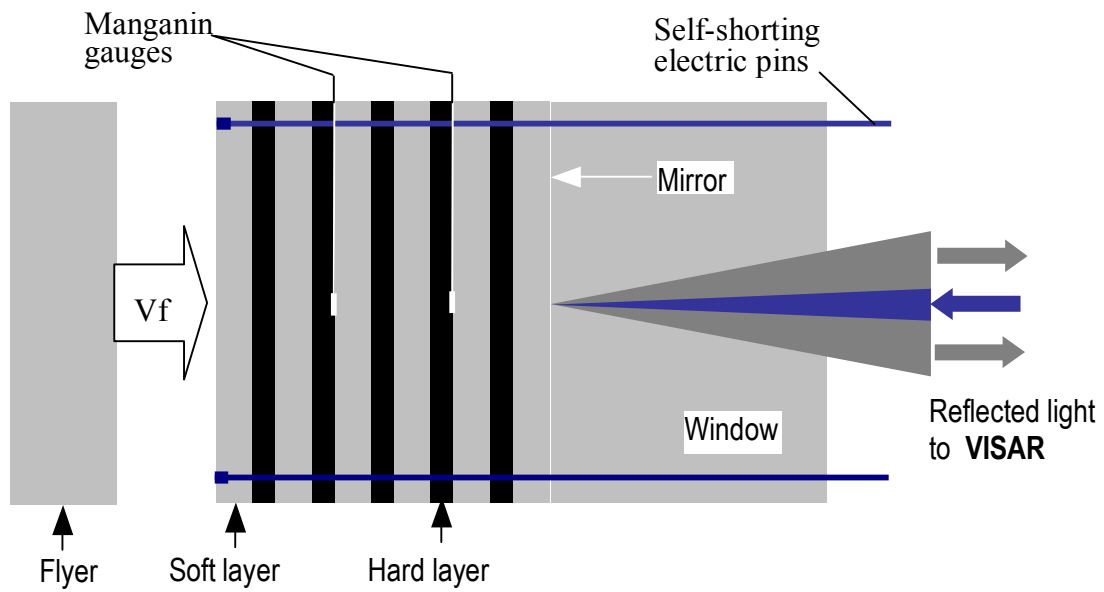
5. List of Figures and Tables

Figure 1. Specimen configuration and schematic of shock compression experiment for periodically layered composite.
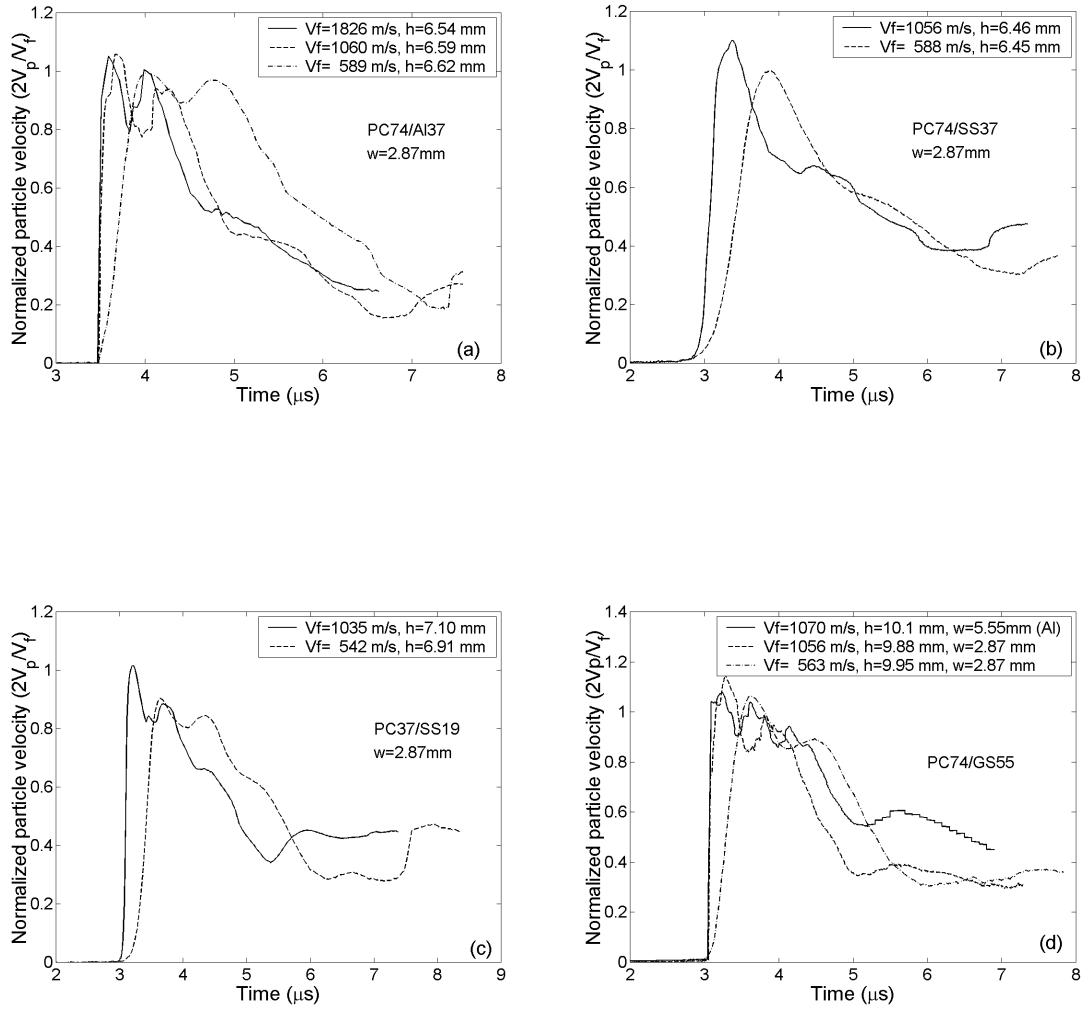Figure 2. Influence of loading amplitude on the shock particle velocity profile for (a) PC74/Al37, (b) PC74/SS37, (c) PC37/SS19 and (d) PC74/GS55 composites. Note, particle velocities are normalized by $V_f/2$; h and w are specimen and flyer thickness, respectively; V_f is the flyer velocity.
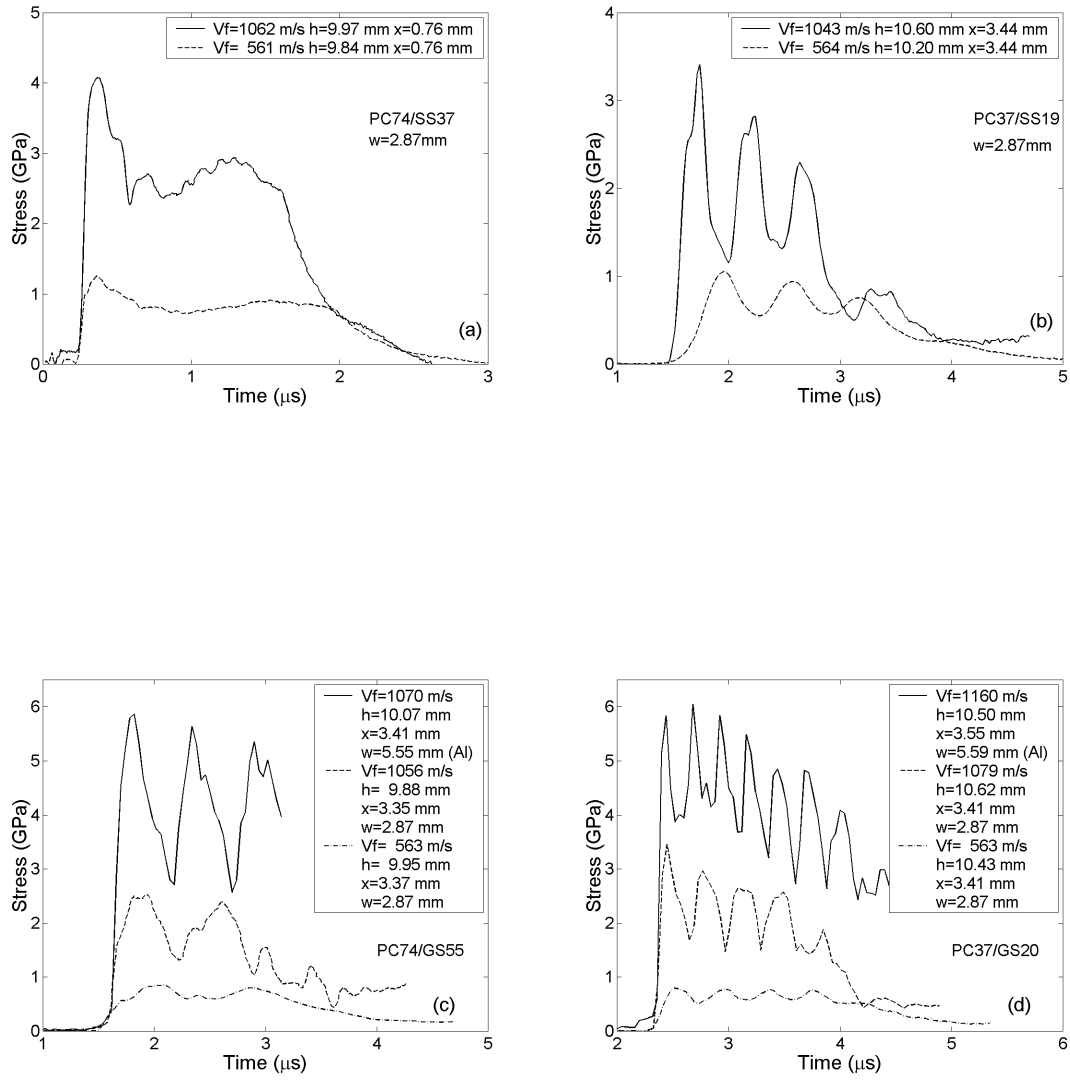Figure 3. Influence of loading amplitude on the shock stress profile for (a) PC74/SS37, (b) PC37/SS19, (c) PC74/GS55 and (d) PC37/GS20 composites. h and w are specimen and flyer thickness, respectively; V_f is the flyer velocity and x is the distance from the impact face.
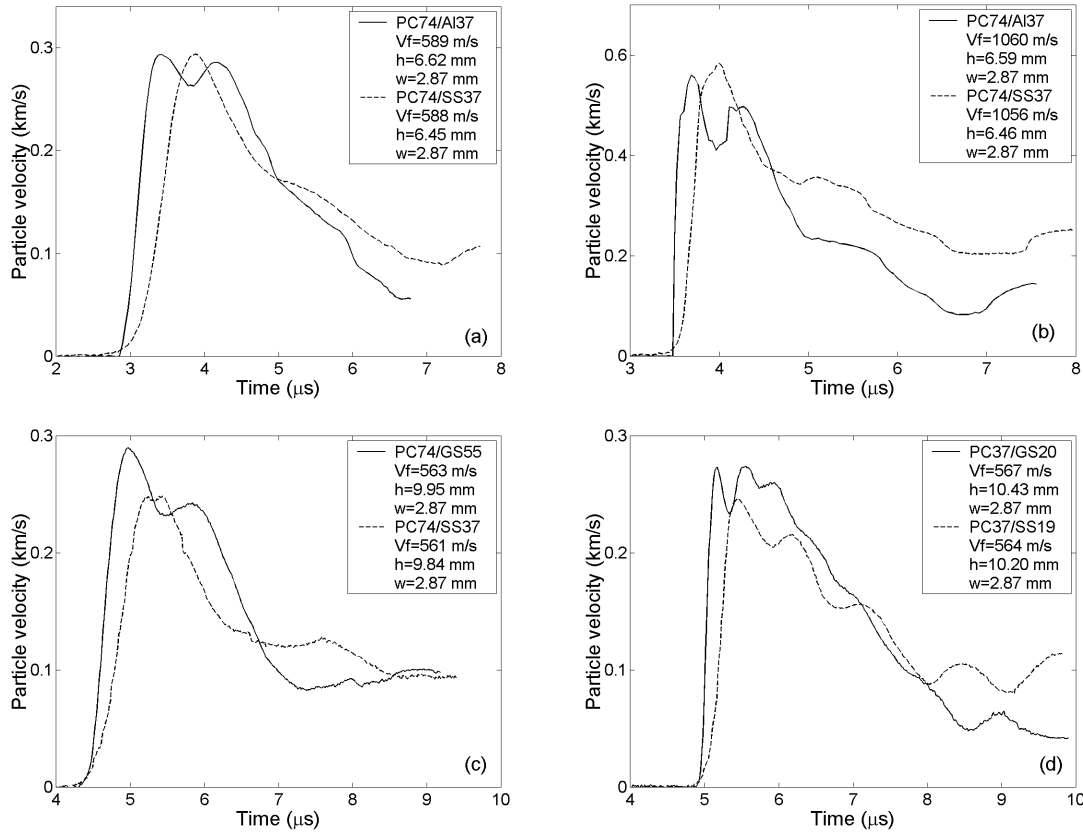Figure 4. Influence of interface mechanical impedance mismatch on shock particle velocity profile for composites PC74/Al37, PC74/SS37, PC74/GS55, PC37/SS19 and PC37/GS20. h and w are specimen and flyer thickness, respectively; V_f is the flyer velocity.
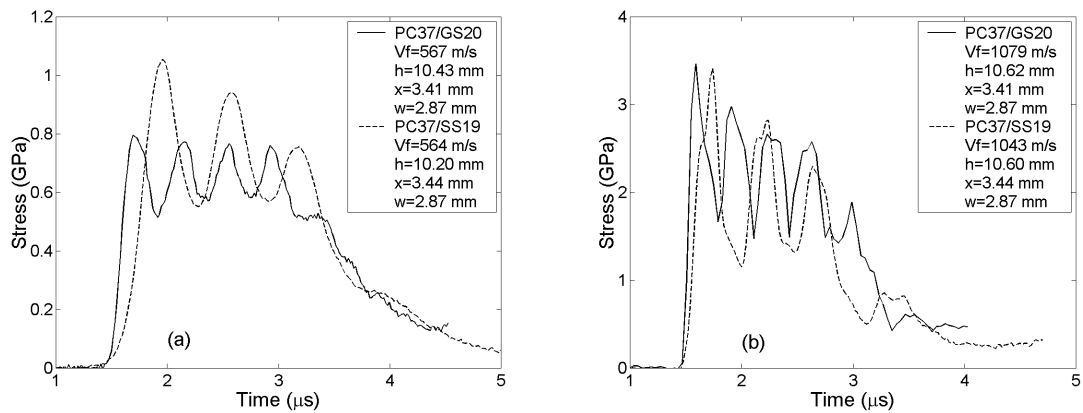Figure 5. Influence of interface mechanical impedance mismatch on shock stress profile for composites PC37/GS20 and PC37/SS19. h and w are specimen and flyer thickness, respectively; V_f is the flyer velocity and x is the distance from impact face.
Figure 6. Influence of interface number on shock particle velocity profile for the PC/SS and PC/GS composites. h and w are specimen and flyer thickness, respectively; V_f is the flyer velocity.
Figure 7. Influence of interface number on shock stress profile for the PC/GS composites. h and w are specimen and flyer thickness, respectively; V_f is the flyer velocity and x is the distance from impact face
Figure 8. Evolution of shock particle velocity profile with propagation distance in PC/SS composites. h and w are specimen and flyer thickness, respectively; V_f is the flyer velocity.
Figure 9. Evolution of shock stress profile with propagation distance in PC37/SS19 composites. h and w are specimen and flyer thickness, respectively; V_f is the flyer velocity and x is the distance from impact face.
Figure 10. Influence of loading pulse duration on the propagation of shock wave in PC37/SS19 composites (velocity profile). h and w are specimen and flyer thickness, respectively; V_f is the flyer velocity.
Figure 11. Influence of loading pulse duration on the propagation of shock wave in PC37/SS19 composite (stress profile).
Figure 12. Influence of release wave on shock particle velocity profile in PC74/GS55 composite.
Figure 13. Comparison of stress profile with velocity profile at an internal interface of 9.95 mm PC74/GS55 composite specimen loaded by 2.87 mm thick PC flyer at velocity of 565 m/s.
Figure 14. Experimental Hugoniot data of PC/GS and PC/SS composites and the comparison with the Hugoniots of their homogeneous component materials.
Figure 15. Shock stress vs. strain rate for the layered composites.

Table 1. Mechanical properties of components for layered composites and window materials.

Table 2. Specimen parameters and the corresponding loading conditions.

Figure 1. Specimen configuration and schematic of shock compression experiment for periodically layered composite.

Figure 2. Influence of loading amplitude on the shock particle velocity profile for (a) PC74/Al37, (b) PC74/SS37, (c) PC37/SS19 and (d) PC74/GS55 composites. Note, particle velocities are normalized by $V_f/2$; h and w are specimen and flyer thickness, respectively; V_f is the flyer velocity.

Figure 3. Influence of loading amplitude on the shock stress profile for (a) PC74/SS37, (b) PC37/SS19, (c) PC74/GS55 and (d) PC37/GS20 composites. h and w are specimen and flyer thickness, respectively; V_f is the flyer velocity and x is the distance from the impact face.

Figure 4. Influence of interface mechanical impedance mismatch on shock particle velocity profile for composites PC74/Al37, PC74/SS37, PC74/GS55, PC37/SS19 and PC37/GS20. h and w are specimen and flyer thickness, respectively; V_f is the flyer velocity.

Figure 5. Influence of interface mechanical impedance mismatch on shock stress profile for composites PC37/GS20 and PC37/SS19. h and w are specimen and flyer thickness, respectively; V_f is the flyer velocity and x is the distance from impact face.

Figure 6. Influence of interface number on shock particle velocity profile for the PC/SS and PC/GS composites. h and w are specimen and flyer thickness, respectively; V_f is the flyer velocity.

Figure 7. Influence of interface number on shock stress profile for the PC/GS composites. h and w are specimen and flyer thickness, respectively; V_f is the flyer velocity and x is the distance from impact face
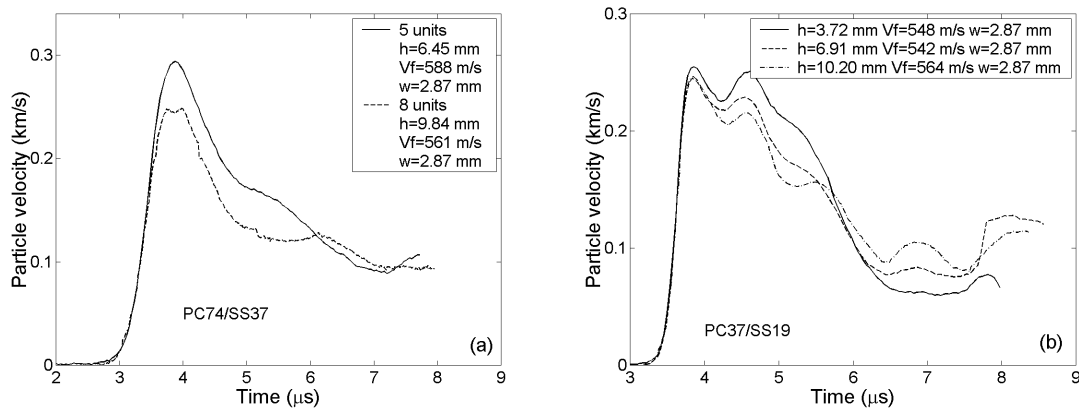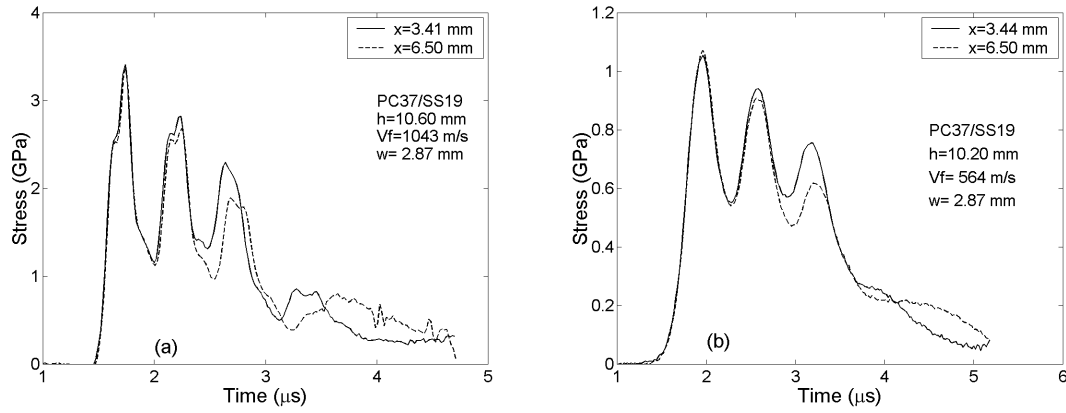
Figure 8. Evolution of shock particle velocity profile with propagation distance in PC/SS composites. h and w are specimen and flyer thickness, respectively; V_f is the flyer velocity.

Figure 9. Evolution of shock stress profile with propagation distance in PC37/SS19 composites. h and w are specimen and flyer thickness, respectively; V_f is the flyer velocity and x is the distance from impact face.
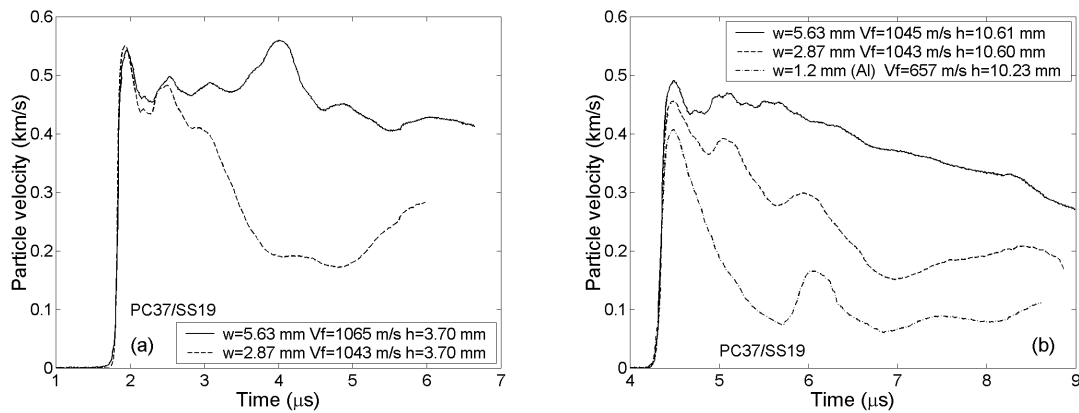

Figure 10. Influence of loading pulse duration on the propagation of shock wave in PC37/SS19 composites (velocity profile). h and w are specimen and flyer thickness, respectively; V_f is the flyer velocity.
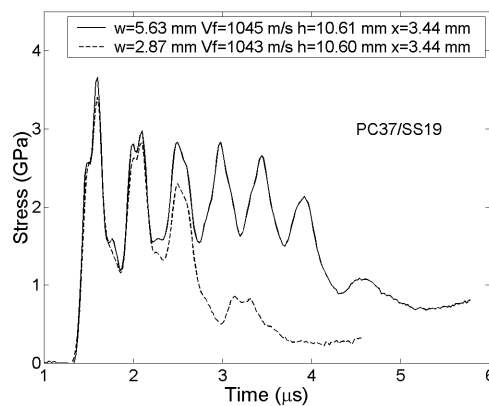

Figure 11. Influence of loading pulse duration on the propagation of shock wave in PC37/SS19 composite (stress profile).
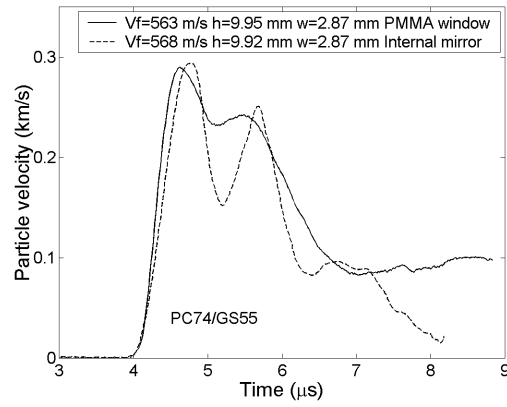
Figure 12. Influence of release wave on shock particle velocity profile in PC74/GS55 composite.
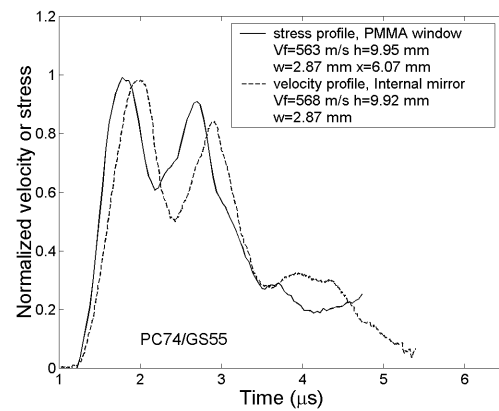

Figure 13. Comparison of stress profile with velocity profile at an internal interface of 9.95 mm PC74/GS55 composite specimen loaded by 2.87 mm thick PC flyer at velocity of 565 m/s.
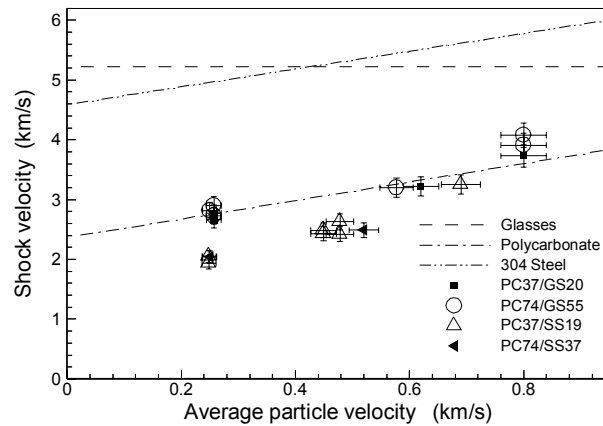

Figure 14. Experimental Hugoniot data of PC/GS and PC/SS composites and the comparison with the Hugoniots of their homogeneous component materials.
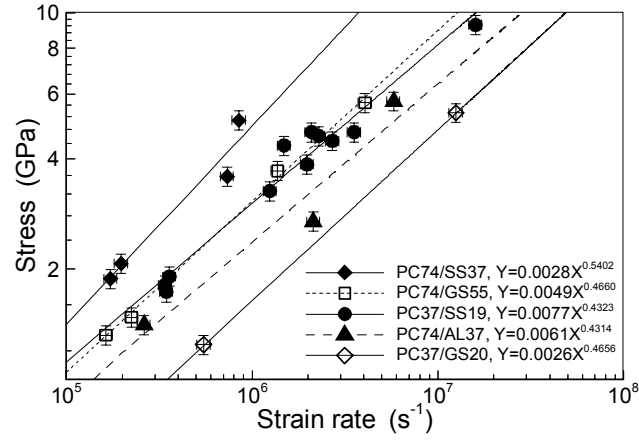
Figure 15. Shock stress vs. strain rate for the layered composites.

Table 1. Mechanical properties of components for layered composites and window materials

Material	ρ (g/cm^3)	G (GPa)	σ_y (GPa)	E_p (GPa)	υ
PC	1.19	0.94	0.00	1.60	0.37
PMMA	1.18	1.20	0.00	1.60	0.34
6061Al	2.71	30.0	0.32	0.69	0.33
304 SS	7.89	77.0	0.33	1.70	0.29
D 263 Glass	2.51	30.1			0.208
Float Glass	2.50	28.2			0.24

Table 2. Specimen parameters and the corresponding loading conditions

Experiment #	Specimen[1] soft/hard	Units	Thickness[2] mm	Flyer velocity m/s	Flyer thickness[3] mm	Gage #1[4] mm	Gage #2[4] mm
072701	PC74/Al37	5	6.59	1060	2.87 (PC)	/	/
072702	PC74/Al37	5	6.62	589	2.87 (PC)	/	/
112902	PC74/Al37	5	6.54	1826	2.87 (PC)	/	/
080301	PC74/SS37	5	6.45	588	2.87 (PC)	/	/
080302	PC74/SS37	5	6.46	1056	2.87 (PC)	/	/
112501	PC74/SS37	8	9.84	561	2.87 (PC)	0.76	/
112502	PC74/SS37	8	9.97	1062	2.87 (PC)	0.76	/
111601	PC37/SS19	16	10.20	564	2.87 (PC)	3.44	6.50
110501	PC37/SS19	16	10.60	1043	2.87 (PC)	3.44	6.50
082201	PC37/SS19	10	6.91	542	2.87 (PC)	/	/
082202	PC37/SS19	10	7.10	1035	2.87 (PC)	/	/
091001	PC37/SS19	5	3.72	548	2.87 (PC)	/	/
091002	PC37/SS19	5	3.70	1043	2.87 (PC)	/	/
103002	PC37/SS19	5	3.77	1589	2.87 (PC)	/	/
102502	PC37/SS19	5	3.70	1065	5.63 (PC)	/	/
102501	PC37/SS19	10	6.94	1076	5.63 (PC)	/	/
110502	PC37/SS19	16	10.61	1045	5.63 (PC)	3.44	9.88
120702	PC37/SS19	16	10.23	657	1.20 (Al)	/	/
111901	PC37/GS20	16	10.43	567	2.87 (PC)	3.41	6.44
112302	PC37/GS20	16	10.50	1160	5.59 (Al)	3.55	3.55
112301	PC37/GS20	16	10.62	1079	2.87 (PC)	3.41	6.44
120201	PC74/GS55	7	9.95	563	2.87 (PC)	3.37	6.07
120202	PC74/GS55	7	9.88	1056	2.87 (PC)	3.35	5.97
120701	PC74/GS55	7	10.07	1070	5.55 (Al)	3.41	6.07
121001	PC74/GS55	7	9.92	568	2.87 (PC)	0.74	/

[1]PC-polycarbonate, Al-6061-T6 aluminum alloy, SS-304 stainless steel; the number following the abbreviation of component material represents the layer thickness in hundredths of a millimeter.

[2]Specimen thickness includes the 0.74 mm PC buffer; the mirror for reflecting the laser to VISAR is located at back surface of the buffer.

[3]Material in parentheses is the flyer material.

[4]The distance of manganin stress gage away from the impact surface.

6. Publications

Grady, D.E., Ravichandran, G., Zhuang, S., 1999. Continuum and subscale modeling of heterogeneous media in the dynamic environment. In: Manghani, M. (Ed.), Proceedings of the AIRPAT Conference, Honolulu, Hawaii. Oxford University Press.

Zhuang, S., 2002. Shock wave propagation in periodically layered composites. *Ph.D. Thesis*, California Institute of Technology.

Zhuang, S., Ravichandran, G., and Grady, D. E., 2002. An Experimental Investigation of Shock Wave Propagation in Periodically Layered Composites, *Journal of the Mechanics and Physics of Solids* (under review).

Zhaung, S., Ravichandran, G. and Grady D. E., 2002. Analysis of Shock Wave Propagation in Periodically Layered Composites", to be submitted to *Journal of Applied Physics*.

7. Scientific Personnel

G. Ravichandran (PI), California Institute of Technology

S. Zhuang (Graduate Student, Ph.D., completed June 2001), California Institute of Technology

D. Grady, Applied Research Associates

8. Bibliography

Asay, J.R., Shahinpoor, M., 1993. High-Pressure Shock Compression of Solids. Springer-Verlag, New York.

Barker, L.M., Hollenbach, R.E., 1970. Shock-wave studies of PMMA, fused silica, and Sapphire. J. Appl. Phys. 41, 4208-4226.

Barker, L.M., 1971. A model for stress-wave propagation. J. Comp. Mat. 5, 140-162.

Barker, L.M., Hollenbach, R.E., 1972. Laser interferometer for measuring high velocities of any reflecting surface. J. Appl. Phys. 43, 4669-4675.

Barker, L.M., Lundergan, C.D., Chen, P.J., Gurtin, M.E., 1974. Nonlinear viscoelasticity and the evolution of stress waves in laminated composites: a comparison of theory and experiment. J. Appl. Mech. 41, 1025-1030.

Ben-Amoz, M., 1975. On wave propagation in laminated composites-II. Propagation Normal to the Laminates. Int. J. Engng Sci. 13, 57-67.

Chen, P.J., Gurtin, M.E., 1973. On the propagation of one-dimensional acceleration waves in laminated composites. J. Appl. Mech. 40, 1055-1060.

Davison, L., Graham, R.A., 1979. Shock compression of solids. Phys. Rep.55, 255-379.

Fraser, D.B., 1968. Factors influencing the acoustic properties of vitreous silica. J. Appl. Phys. 39, 5868-5878.

Grady, D.E., Ravichandran, G., Zhuang, S., 1999. Continuum and subscale modeling of heterogeneous media in the dynamic environment. In: Manghani, M. (Ed.), Proceedings of the AIRPAT Conference, Honolulu, Hawaii. Oxford University Press.

Johnson, J.N., Barker, L.M., 1969. Dislocation dynamics and steady plastic wave profiles in 6061-T6 aluminum. J. Appl. Phys. 40, 4321-4334.

Johnson, J.N., 1992. Calculation of path-dependent wave shock hardening. J. Appl. Phys. 72, 797-799.

Johnson, J.N., Hixson, R.S., Gray, G.T.III, 1994. Shock-wave compression and release of aluminum/ceramic composites. J. Appl. Phys. 76, 5706-5718.

Kanel, G.I., Ivanov, M.F., Parshikov, A.N., 1995. Computer simulation of the heterogeneous materials response to the impact loading. Int. J. Impact Engng. 17, 455-464.

Lundergan, C.D., Drumheller, D.S., 1971. Dispersion of shock waves in composite materials. In: Burke, J. and Weiss, V. (Ed.), Shock Waves and the Mechanical Properties of Solids. Syracuse University Press, New York, 141-154.

Marsh, S.P., 1980. LASL shock Hugoniot data. University of California Press, California.

Meyers, M.A., 1994. Dynamic Behavior of Materials. John Willey & Sons, Inc., New York.

Mutz, A.H., 1991. Heterogeneous Shock Energy Deposition in Shock Wave Consolidation of Metal Powders. Ph.D. Thesis, California Institute of Technology.

Nayfeh, A.H., 1995. Wave Propagation in Layered Anisotropic Media: with Applications to Composites. Elsevier Science, Amsterdam.

Oved, Y., Luttwak, G.E., Rosenberg, Z., 1978. Shock wave propagation in layered composites. J. Comp. Mat. 12, 84-96.

Partom, Y., 1990. Understanding the Swegle-Grady fourth power relation. In: Schmidt, S.C., Johnson, J.N., Davison, L.W. (Ed.), Shock Waves in Condensed Matter-1989. American Institute of Physics, New York, 317-320.

Rubin, M.B., 1990. Analysis of weak shocks in 6061-T6 aluminum. In: Schmidt, S.C., Johnson, J.N., Davison, L.W. (Ed.), Shock Waves in Condensed Matter-1989. American Institute of Physics, New York, 321-328.

Schuler, K.W., Nunziato, J.W., 1974. The dynamic mechanical behavior of polymethyl methacrylate. Rheol. Acta 13, 265-273.

Sun, C.T., Achenbach, J. D., Hermann, G., 1968. Continuum theory for a laminated medium. J. Appl. Mech. 35, 467-475.

Swegle, J.W., Grady, D.E., 1985. Shock viscosity and the prediction of shock wave rise times. J. Appl. Phys. 58, 692-701.

Wackerle, J., 1962. Shock-wave compression of quartz. J. Appl. Phys. 33, 922-937.

Zhuang, S., 2002. Shock wave propagation in periodically layered composites. Ph.D. Thesis, California Institute of Technology.

MEMORANDUM OF TRANSMITTAL

U.S. Army Research Office
ATTN: AMSRL-RO-BI (TR)
P.O. Box 12211
Research Triangle Park, NC 27709-2211

☐ Reprint (Orig + 2 copies)   ☐ Technical Report (Orig + 2 copies)

☐ Manuscript (1 copy)   ☒ Final Progress Report (Orig + 2 copies)

☐ Related Materials, Abstracts, Theses (1 copy)

CONTRACT/GRANT NUMBER: **DAAG55-98-1-0237**

REPORT TITLE: Stress Wave Propagation Through Heterogeneous Media

is forwarded for your information.

SUBMITTED FOR PUBLICATION TO (applicable only if report is manuscript):

Sincerely,

G. Ravichandran
California Institute of Technology
Graduate Aeronautical Laboratories
Pasadena, CA 91125